Global and Planetary Change 145 (2016) 67–77

Contents lists available at ScienceDirect

Global and Planetary Change

journal homepage: www.elsevier.com/locate/gloplacha

Invited research article

Historical analysis and visualization of the retreat of Findelengletscher, Switzerland, 1859–2010

P. Rastner [a,*], P.C. Joerg [a], M. Huss [b,c], M. Zemp [a]

[a] Department of Geography, University of Zurich, Switzerland
[b] Department of Geosciences, University of Fribourg, Switzerland
[c] Laboratory of Hydraulics, Hydrology and Glaciology (VAW), ETH Zurich, Switzerland

ARTICLE INFO

Article history:
Received 25 February 2016
Received in revised form 6 July 2016
Accepted 15 July 2016
Available online 28 July 2016

Keywords:
Glacier
Historical maps
DEMs
Computer animation
Public communication of science

ABSTRACT

Since the end of the Little Ice Age around 1850, glaciers in Europe have strongly retreated. Thanks to early topographic surveys in Switzerland, accurate maps are available, which enable us to trace glacier changes back in time. The earliest map for all of Switzerland that is usable for a detailed analysis is the Dufour map from around 1850 with subsequent topographic maps on a ~20 year interval. Despite the large public and scientific interest in glacier changes through time, this historic dataset has not yet been fully utilized for topographic change assessment or visualization of historic glacier extents. In this study, we use eleven historical topographic maps and more recent digital datasets for the region of Zermatt to analyze geometric changes (length, area and volume) of Findelengletscher as well as for creating animations of glacier evolution through time for use in public communication. All maps were georeferenced, the contour lines digitized, and digital elevation models (DEMs) created and co-registered. Additional digital data like the SRTM X-band DEM and high resolution laser scanning data were used to extend the analysis until 2010. Moreover, one independent DEM from aerial photogrammetry was used for comparison. During the period 1859–2010, Findelengletscher lost 3.5 km of its length (6.9 km in 2010), 4.42 ± 0.13 km^2 of its area (15.05 ± 0.45 km^2 in 2010) and 1.32 ± 0.52 km^3 of its volume. The average rate of thickness loss is 0.45 ± 0.042 m yr^{-1} for the 151 years period. Four periods with high thickness change from −0.56 m ± 0.28 yr^{-1} (1859–1881), −0.40 ± 0.08 m yr^{-1} (1937–1965), −0.90 ± 0.31 m yr^{-1} (1995–2000) and −1.18 ± 0.02 m yr^{-1} (2000–2005) have been identified. Small positive thickness changes were found for the periods 1890–1909 (+0.09 ± 0.46 m yr^{-1}) and 1988–1995 (+0.05 ± 0.24 m yr^{-1}). During its retreat with intermittent periods of advance, the glacier separated into three parts. The above changes are demonstrated through an animation (available from the supplementary material), which has been created to inform the general public.

1. Introduction

Glaciers are sensitive indicators for climatic variations. Understanding the evolution and spatial variability of glaciers may thus contribute to better knowledge of impacts, trends and rates of ongoing climate change. Rates and ranges of such fluctuations in the past can be, for example, retrieved from topographic maps and thus contribute to our understanding of the glacier-climate linkage (Bauder et al., 2007; Finsterwalder and Rentsch, 1980; Fischer, 2011; Hoinkes, 1970; Huss et al., 2010). The first geometrically accurate topographic map of Switzerland, the Dufourkarte (in the following referred as Dufour map), was published between 1844 and 1864 (Graf, 1896; Wolf, 1879) and provides an important baseline dataset obtained close to the Little Ice Age (LIA) maximum extent of glaciers in the Alps. Since then, maps in Switzerland have been continuously improved and updated in a ~10–20 year interval. Nowadays, this historical data offers a unique pool of information, which can be used to assess landscape evolution from both a qualitative and quantitative point of view. In the particular case of a glacier, historical maps allow retrieving, besides the former length and area (Haggren et al., 2007; Maisch et al., 2000), also its former surface topography, when elevation contour lines are provided. In the recent past, several studies have utilized historic topographic maps for the calculation of glacier elevation and volume changes (Bauder et al., 2007; Junfeng et al., 2015; Surazakov and Aizen, 2006; Xu et al., 2013). Most of these studies, however, have first of all not used a complete series of topographic maps covering a 150-year period in high temporal resolution and secondly not visualized the glacier changes for a wider public. Given that the information in these maps is digitally available, it is thus possible to assess glacier changes quantitatively and qualitatively to create dynamic 3-D visualizations with current computer hard and software (Wang et al., 2006).

* Corresponding author.
E-mail address: philipp.rastner@geo.uzh.ch (P. Rastner).

http://dx.doi.org/10.1016/j.gloplacha.2016.07.005
0921-8181/

The aims of this study are to (1) utilize historic topographic maps for the calculation of glacier changes in length, area and volume, (2) the assessment of related uncertainties, and (3) visualization of the changes over time using 3D computer animation to (a) bridge temporal gaps between the map sheets and (b) provide a visually attractive rendering of the changes for enhanced public communication.

2. Study region

Findelengletscher is a large temperate valley glacier located in the Swiss Alps (46° 00′ N, 7° 52′ E) in the Canton Valais, close to the village of Zermatt and at the border to Italy (Fig. 1). The glacier had an area of 13.0 km^2 and a length of 6.7 km in 2010 (Joerg et al., 2012). It is exposed to the Northwest and covers an elevation range from 2600 m a.s.l. up to 3900 m a.s.l. Most of the precipitation on Findelengletscher is advected from South and Southeast (Sold et al., 2013). The current equilibrium line altitude is at between 3200 and 3300 m a.s.l. and thus one of the highest in the Alps (Huss et al., 2014; Maisch et al., 2000). Since its LIA maximum extent around 1850, the glacier retreated and separated in 1990 from its former tributary Adlergletscher. Length change or front variation measurements started in 1885 (Glaciological reports (1881–2016), 2016), whereas direct glaciological mass balance measurements were initiated in 2004 (Machguth, 2008; Sold et al., 2016).

3. Data

3.1. Topographic maps

All topographic maps were ordered from the Swiss Federal Office of Topography (Swisstopo) in digital format. The six oldest ones, however, were without projection information. Due to the large variability in the applied map updates, the selection of appropriate maps was crucial for the current work. We decided to use only maps, which resolve observed periods of glacier advance or recession (extent, contour lines). A challenge in this regard was the exact dating of the maps as acquisition and publication years differ. The acquisition year was determined from the map itself if mentioned, or it was retrieved from the Alexandria Catalogue (http://www.alexandria.ch), a portal that hosts historical Swiss documents, if available. In total, eleven different releases of historical maps dating back to the earliest map available for the Zermatt region were collected to derive length, area and volume changes of Findelengletscher (Table 1). The first historical document used was the Dufour map (map sheet 23, Section 5 and number 495), featuring a complete and accurate representation of the complex topography of Switzerland and already at its time regarded as a masterpiece of cartography. The geodetic reference system of the Dufour maps were geodetic triangulation points (first-order reference points) established through a network of surveyed triangles over the whole of Switzerland. Starting with these reference points with known coordinates and elevations, the surveyors were able to perform detailed topographic measurements using plane tables according to instructions from General Dufour (Graf, 1896). An analysis from Rickenbacher (2009) on an excerpt of the Dufour map revealed an average horizontal deviation of 153 m in natura of 2560 points in the map.

To determine the elevation above sea level, a point of origin for elevation measurements was defined in the harbour of Geneva (Pierre du Niton; 376.2 m above sea level = 'old horizon') and levelled to the reference points and other topographically important features (e.g. summits, lake levels etc.). The reference system of the Dufour map is CH1840 with equivalent conical projection. The Dufour map could only be used for determining glacier area and length as no contour lines are depicted. However, contour lines (30 m equidistance) were derived from the corresponding plane-table sheet (Messtischblatt) from 1859 recorded by the cartographer Betémps (Holzhauser, 2010; Steiner et al., 2008). We further selected five maps from the Siegfried

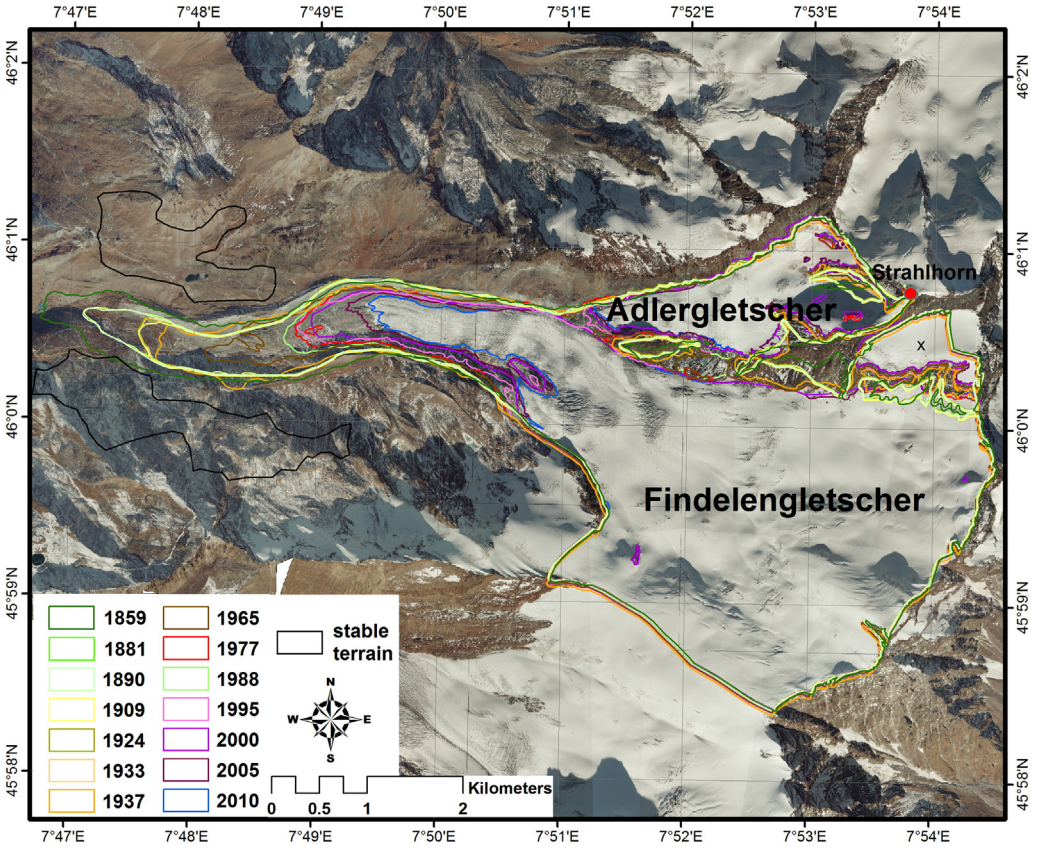

Fig. 1. Orthoimage of Findelen- and Adlergletscher from 2005 including historical outlines and the area (stable terrain) used for the co-registration of the DEMs.

Table 1
Dataset overview and their properties for the calculation of changes in length, area and volume of Findelengletscher. Note the 1982 independent DEM was only used for data comparisons. The last column shows the data voids for map derived DEMs in percent.

Acquisition year	Publication year	Map name/dataset	Contour lines aequidistances	Scale	Contour lines & glacier outlines ablation area	Contour lines accumulation area	Data voids in %
1859	1862	Plane table sheet	30	1:50,000	New	New	33
No info	1881	Siegfried map	30	1:50,000	Updated	Updated	24
No reference	1890	Siegfried map	30	1:50,000	Identical	Identical	26
No reference	1909	Siegfried map	30	1:50,000	Updated	Identical	24
1924	1926	Siegfried map	30	1:50,000	Identical	Identical	24
1933	1935	Siegfried map	30	1:50,000	Identical	Identical	26
1937	1941	Old national map	20	1:50,000	Updated	Updated	8
1965	1966	National map	20	1:25,000	Updated	Updated	8
1977	1980	National map	20	1:25,000	Updated	Identical	4
1988	1993	National map	20	1:25,000	Updated	Identical	9
1995	1998	National map	20	1:25,000	Updated	Identical	4
2000	2000	SRTM X-band DEM	25 m res.	–	New	New	–
28/29 oct. 2005	2005	Laserscan DEM	1 m res.	–	New	New	–
29 sep. 2010	2010	Laserscan DEM	1 m res.	–	New	New	
1982 ind. DEM	1982	Aerial photogrammetry	25 m res.	–	New	New	–

map series, of the years 1881, 1890, 1909, 1924, and 1933 with 30 m elevation contours and the same geodetical properties as the Dufour map (Oberli, 1968). In the late 1930s, the Dufour and Siegfried maps were superseded by the newly developed national maps. With this new map series, the reference system changed to CH1903 with conformal oblique cylinder projection. Moreover, the point of origin for elevation measurements changed to 373.6 a.s.l. (i.e. the 'new horizon') and contour lines of 20 m were introduced. In the 1960s, land surveys by airborne photogrammetry were initiated, which allowed the production of topographic maps (national maps) at a 1:25,000 scale (1965, 1977, 1988, and 1995). Improvements in surveying and photogrammetric methods have thus resulted in an increasing accuracy over time.

Contour lines, however, especially in the accumulation region of a glacier, were not updated as frequently as the contour lines and the extent at the glacier tongue. After the initial plane-table sheet, updated contour lines and new glacier front position were available for the first time on the map of 1881 for the entire glacier. The map from 1890 shows no changes of the contour lines compared to 1881. In 1909, the front position was updated with only slight changes of the contours on the tongue, whereas for 1924 and 1933 they remained the same, likewise, the glacier geometry. With the introduction of the national map in 1937, glacier front position and contour lines were updated on the whole of the glacier. The same is applicable for the national map of 1965, however, in 1977, 1988, and 1995, only the glacier front position and new contour lines in the ablation area of the glacier were drawn (Table 1).

3.2. Digital elevation models

For the year 2000, we used the Shuttle Radar Topography Mission (SRTM) digital elevation model (DEM) (Jarvis et al., 2008). The SRTM DEM is widely used in glacier change assessments (Paul and Haeberli, 2008; Schiefer et al., 2007; Surazakov and Aizen, 2006) and it thus provided a good opportunity to assess its potential for glacier thickness change assessments. The SRTM DEM was acquired by radar interferometry (InSAR) during 10 days in February 2000, when a Space Shuttle mapped the Earth's surface between 60°N and 56°S with C- and X-band radar. It has been suggested that SRTM derived DEMs underestimate glacier elevation, due to considerable penetration of the radar waves into the winter snowpack (Gardelle et al., 2013). However, the penetration depth of the here used X-band wavelength is not expected to be as pronounced as in SRTM C-band (Dehecq et al., 2016; Rignot et al., 2001) which is an advantage for the volume change calculations. Moreover, the relative vertical accuracy is lower for the SRTM C-band (10 m) than for the SRTM X-band (6 m) (Hoffmann and Walter, 2006). We therefore decided to use the SRTM X-band DEM, which was available void free for the region of Zermatt and downloaded it from the German Aerospace Center earth observation on the web (EOWEB) platform (Farr et al., 2007). It is worthwhile to mention that both SRTM products refer to different vertical datums. The C-band product refers to the EGM96 (Earth Gravitational Model 1996) geoid, whereas the X-band product refers to the WGS84 (World Geodetic System 1984) ellipsoidal vertical datum (Hoffmann and Walter, 2006). As elevations in Swiss maps refer to the geoid, the geoid undulation to the X-band SRTM ellipsoid elevations had to be taken into account. The horizontal variability in the geoid undulation remains below a few centimeters per kilometer in the region of Findelengletscher. Hence, we decided to keep the original ellipsoid elevations to be globally corrected by the co-registration pre-processing step explained in Section 4.1.3. For 2005 and 2010, we used two high resolution airborne laser-scanning DEMs with identified high accuracies collected in the framework of the Glacier Laserscanning Experiment Oberwallis (GLAXPO) project (Joerg et al., 2012). These laser-scanning campaigns were performed with the Optech ALTM 3100 system and resulted in DEMs of 1 m spatial resolution (Joerg et al., 2012). In addition, one DEM created by aerial photogrammetry for 1982 with a spatial resolution of 25 m was available from Bauder et al. (2007) which was used for comparison with the results of this study (Table 1).

3.3. Imagery

Two images served as base dataset for the visualization (Table 1). The first one was an aerial image with 0.5 m resolution collected in the GLAXPO project (Joerg et al., 2012). The second image was a Landsat 7 ETM+ level 1T (path: 195, row: 028) satellite scene acquired on 12.08.2000 with 30 m resolution (downloaded from the USGS Earth Explorer http://earthexplorer.usgs.gov/).

4. Methods

The methods can be divided into four parts. First, the raw data input preparation, second, the uncertainty assessment, third, the data preparation for the computer animation, and finally the rendering and movie editing (c.f. Fig. 2). All data pre-processing and main processing were performed in the ENVI 4.7 remote sensing and IDL programming software (Exelis Visual Information Solution, USA). Esri ArcGIS 10.2 and Microsoft Excel were used for the co-registration and Adobe Photoshop for the DEM void filling and artefact removal. The DEM morphing was done in Abrosoft Fanta Morph and the rendering of the computer animation in Visual Nature Studio 3 (VNS; 3D Nature LLC). Finally, all movie components were matched together in the video editing program Adobe Premiere.

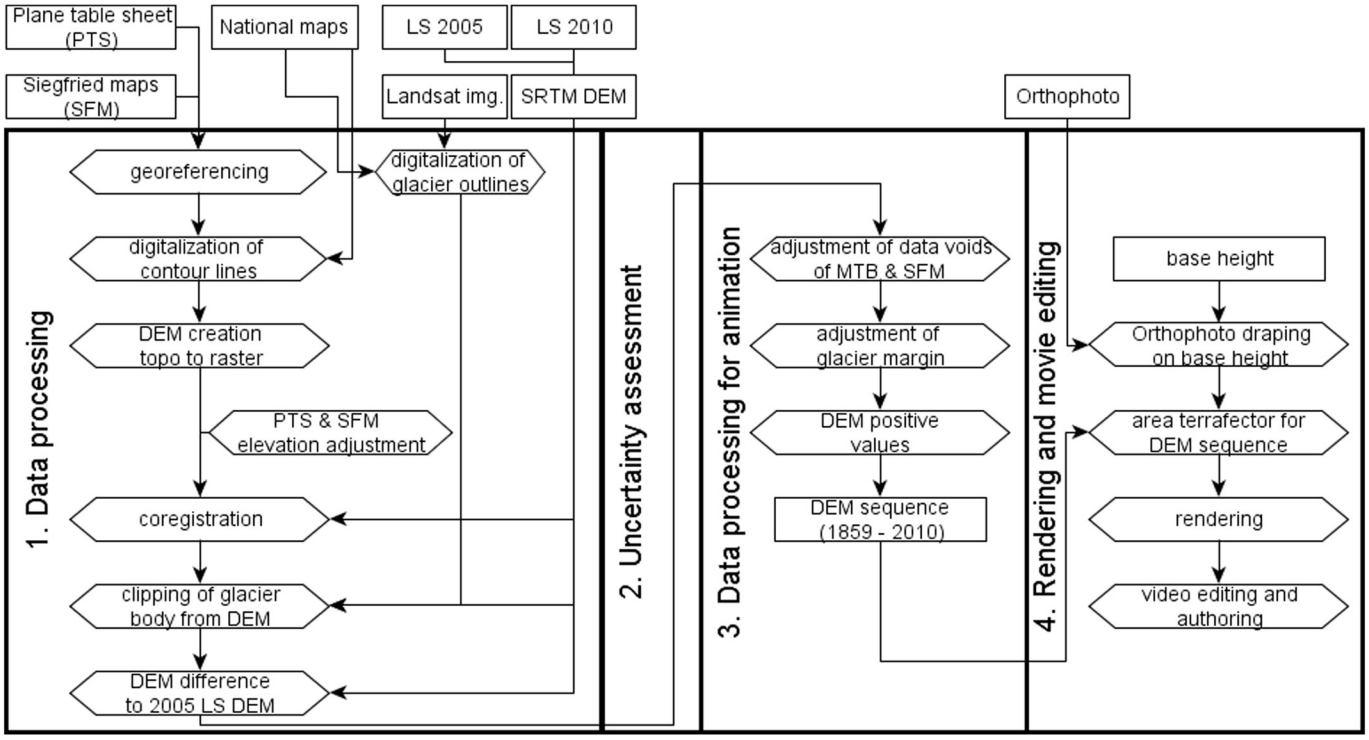

Fig. 2. Processing flow chart.

4.1. Raw data input preparation

4.1.1. Georeferencing

The first step was to georeference the plane-table sheet and all Siegfried maps in a common reference system. The georeferencing was challenging for the plane table sheet as ground control points (GCPs) had to be identified. This was often hampered as few reference points on the ground remained the same and were visible during the 150-year period. For the Siegfried maps, as the then-established map grids remained the same through the years, tie points could be used instead. This work step resulted in five georeferenced maps in UTM 32 WGS 84 map projection, which was used as standard projection throughout this work. The highest root-mean-square (RMS) error occurred during the georeferencing of the plane table sheet (~4 m), whereas for the Siegfried maps it was only around ~1 m (Table 2).

4.1.2. Digitization of contour lines and glacier outlines

In this study, we decided to digitize contour lines above the glacier surface and surrounding terrain (hereafter called stable terrain) instead of only using contour points. The usage of contour points would lead to an underestimate of the glacier surface, as they tend to be more numerous towards the edges of the glacier (due to the curvature of the contour) and less in the centre (Nuth et al., 2007). Contour lines were manually digitized on a scale of about 1:10,000 and designated with the respective elevation value of the map in the attribute table of the shapefile. This work step was laborious in steep terrain, when elevation contour lines are close to each other. Finally, DEMs were created from the contour lines using the "topo to raster" interpolation function in ArcGIS 10 with a resolution of 25 m. Because the origin of elevation has changed from the old horizon to the new horizon, the z-values of the historical DEMs (1859–1933) have been corrected by − 3 m to obtain a comparable dataset (Gubler, 2011; Kobold, 1983). Historical glacier outlines were manually digitized based on the original georeferenced map datasets. For the year 2000, a Landsat satellite image was used to derive the glacier outline.

Table 2
Total root mean square (RMS) error and number of ground control points (GCP)/TIE points used for the georeferencing of six historical maps.

Years	Map name/dataset	Total RMS error	Nr. of GCP/TIE points
1859	Plane-table sheet	4.08	10
1881	Siegfried map	1.28	35
1890	Siegfried map	0.87	40
1909	Siegfried map	0.89	69
1924	Siegfried map	1.31	69
1933	Siegfried map	1.39	69

4.1.3. Co-registration of DEMs

To increase the accuracy in x, y and z direction, all DEMs were co-registered according to the method of Nuth and Kääb (2011). This step was facilitated by the availability of the high-resolution laser-scanning DEM from 2005 (in the following referred as reference DEM) representing the glacier surface and the surrounding terrain. A potential systematic horizontal shift and/or vertical offset between any historical DEM and the reference DEM was determined by dividing the differences in the raster cell elevation by the tangent of the local slope and a plot against the local aspect for a defined area of stable terrain close to the glacier. The stable terrain has an area of 2.9 km^2, an elevation range of 680 m, a mean slope of 23° and a predominantly north facing aspect direction in our case (Fig. 1, black outlines). A cosine function was fitted by a least-squares curve fit to derive the parameters magnitude m and direction of the horizontal shift d, as well as a mean vertical bias ($\overline{dh}_{terrain}$) (Nuth and Kääb, 2011). Subsequently, all historical DEMs and the independent DEM from 1982 were iteratively shifted and the co-registration was re-assessed. For the 1859 and 2000 DEMs, two iterations, and for all other DEMs only one iteration was necessary to achieve sub-pixel accuracy. No co-registration was necessary for the laser-scanning DEMs from 2005 and 2010 as their localisation accuracy was already high (Joerg et al., 2012) (Table 3). After the co-registration, also the glacier outlines were shifted according to the co-registration shift vectors.

Table 3
Co-registration details for each DEM relative to the 2005 DEM. Δx, y and z are the shift vectors, the standard deviation (*STDEV*) & the mean (median) $\overline{dh}_{terrain}$ Δz on stable terrain before and after the co-registration.

	Δx	Δy	Δc	*STDEV* (before)	*STDEV* (after)	$\overline{dh}_{terrain}$ before [m]	$\overline{dh}_{terrain}$ after [m]
1859	47.8	−50.8	−41.4	32.5	25.4	45.06 (43.4)	−5.59 (−3.5)
1859*	19.7	5.4	9	25.4	24.6	−5.59 (−3.5)	0.8 (2.8)
1881	29.7	8.6	1	34.7	34.2	1.44 (3.7)	0.06 (2.8)
1890	38	11.9	0.4	35.3	34.2	3.08 (6.2)	1.13 (4.7)
1909	30.9	−3.1	2.8	35.5	35	1.91 (1.7)	1.64 (1.5)
1924	30.3	22.4	1	35.3	35	1.95 (2.1)	1.8 (1.5)
1933	38.1	11.8	−0.4	34.3	33.4	3.08 (6.7)	0.29 (3.8)
1937	−4.8	−34	−0.9	15.2	11.4	3.69 (7.6)	0.21 (−1.1)
1965	−7.2	−18.2	−1.9	8.72	7.49	3.01 (3.6)	1.08 (0.4)
1977	−6.9	−18	−2.1	8.77	7.7	3.15 (3.6)	1.06 (0.4)
1988	−7	−17.9	−2.1	8.7	7.71	3.13 (3.6)	1.05 (0.4)
1995	−7.6	−20.8	−1.7	9.73	6.97	2.98 (4)	1.27 (0.9)
2000	40.6	−51.1	−61.1	19.54	11.14	58.65 (60.6)	−13.12 (−12.6)
2000*	−27.7	6.9	6.7	11.14	8.53	−13.12 (−12.6)	−2.35 (−2.3)
1982+	0.9	−18.9	0	9.3	5.6	−0.7 (−0.2)	0.14 (0.04)

* 2nd iteration.
\+ independent DEM.

4.1.4. Glacier changes in length, area and volume

The length of Findelengletscher was derived by manually digitizing a central flowline connecting the highest and lowest point with a maximum distance to the glacier margins and respecting downhill flow (Machguth and Huss, 2014). Changes in area were assessed with the aid of a shapefile polygon feature of the respective year in a GIS system. Changes in volume were calculated from DEM differencing. In particular for DEM differences earlier than 1937, regions were detected (regions which are not well visible from the valley floor), that implied that the historical glacier surface was lower than the 2005 glacier surface (compare also Figs. 4 & 5). Due to strong glacier retreat and mass loss over the 20th century, this is assumed to be erroneous and thus a data void (cf. Table 1). We developed therefore, a method to assess the historical volume changes by accounting for areas that are thought to be surveyed wrong, in particular, in the accumulation region of the glacier. We rely, therefore, on a hypsometric interpolation by excluding all data voids, and using a mean thickness change value from the same hypsometric altitude of one time stamp to fill data voids. To do so, we (1) classified the glacier in 100 m elevation intervals (Fig. 3). In a second step, we calculated a difference grid of each historical DEM to the reference grid of 2005. In a further step, we determined average elevation change over the part of each 100 m elevation interval that indicates surface lowering over time, and, hence, a realistic ice surface evolution. For elevation intervals with data voids (Fig. 3, 4a), we retrieved the area related to data voids (4b) and multiplied this area by the average elevation change (4c, 4d) as retrieved in step (4a). Summing all volume changes per elevation band then leads to the overall volume change. This workflow was performed for each elevation interval with data voids, and for each co-registered DEMs derived from historical topographic maps.

4.2. Uncertainty assessment

The uncertainty of glacier outlines is difficult to assess as appropriate reference data is often missing. For a debris-free glacier like Findelengletscher the precision of the outlines in former studies were found to be about 30 m studies (one Landsat pixel) (Bolch et al., 2010; Paul et al., 2013; Rastner et al., 2012). We thus determined the precision by applying ±15 m buffer around Findelengletscher. Adding this uncertainty gives a ±3% larger total area, which is in the following used as a measure of uncertainty for the glacier area. The same precision (±15 m) was assumed to describe the length uncertainty (due to scale independency the uncertainty for length is not explicitly mentioned in the following).

The mean elevation difference over stable terrain ($\overline{dh}_{terrain}$) between two elevation data sets can be considered as the systematic uncertainty for the glacier's average thickness and volume changes. We therefore defined an area which is ice-free (stable) throughout the 151 years (see Fig. 1). The systematic uncertainty is then calculated

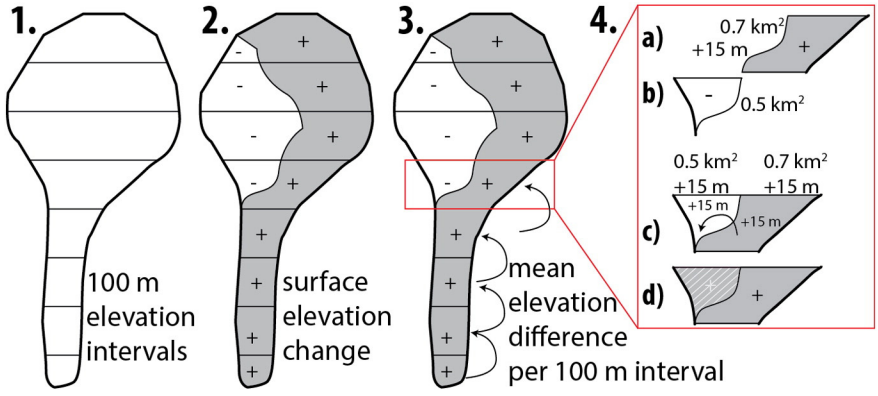

Fig. 3. A schematic illustration of how historical volume changes have been calculated. Realistic thickness values (grey) and data voids are shown in white color, which are assumed to be data voids.

Table 4
Glacier length and area as well as volume and elevation changes in relation to the reference DEM from 2005.

Year	Length [km]	Area +/- [sigma] [km^2]	Δv (rel. 2005) +/- [sigma] [km^3]	Δv per year (rel. 2005) +/- [sigma] [10^{-3} km^3 yr^{-1}]	[Δ]h (rel. 2005) +/- sigma [m]
1859	10.43	19.47 ± 0.58	−1.29 ± 0.47	−8	−65.6 ± 6.25
1881	9.98	18.44 ± 0.55	−0.85 ± 0.63	−6	−52.3 ± 8.83
1890	9.96	18.41 ± 0.55	−0.82 ± 0.62	−7	−50.4 ± 8.90
1909	9.34	18.21 ± 0.54	−0.84 ± 0.63	−8	−51.1 ± 9.35
1924	9.34	18.34 ± 0.55	−0.84 ± 0.64	−10	−50.7 ± 9.44
1933	9.33	18.24 ± 0.54	−0.81 ± 0.60	−11	−49.2 ± 9.01
1937	9.09	18.22 ± 0.54	−0.40 ± 0.20	−6	−28.8 ± 2.44
1965	8.63	17.15 ± 0.51	−0.21 ± 0.12	−5	−17.3 ± 1.57
1977	7.63	16.81 ± 0.50	−0.22 ± 0.12	−7	−16.1 ± 1.70
1988	7.77	16.87 ± 0.50	−0.18 ± 0.13	−10	−14.3 ± 1.69
1995	7.60	16.43 ± 0.49	−0.19 ± 0.11	−19	−13.6 ± 1.56
2000	7.48	15.89 ± 0.47	−0.10 ± 0.13	−20	−5.8 ± 0.14[a]
2005	7.11	15.34 ± 0.46	Reference	Reference	Reference
2010	6.90	15.05 ± 0.45	0.03 ± 0.05	6	3.4 ± 0.20[a]

[a] All pixel values with co-registration.

by taking the mean of the subtraction of the slave minus the master DEM ($\overline{dh}_{terrain}$, Table 3, last column). The elevation variability over stable terrain can be considered as an estimate for the stochastic uncertainty (σ) from one map dataset to another. For DEMS acquired in 2000 and 2010 all pixel values were considered ($\overline{dh}_{glacierized}$; Table 5, second column). The sum of column one and two in Table 5 gives the average thickness change from one map dataset to another ($\overline{dh}_{glacierized} + \epsilon$; Table 5, column 4). Afterwards, the number of contour lines (n) intersecting the polygon of Findelengletscher of the respective year were counted (minimum 62, maximum 91). Due to the fact that there is considerable spatial autocorrelation in the map derived DEMs (Joerg et al., 2012; Joerg and Zemp, 2014), we account for this by calculating the stochastic uncertainty with the 'low' number of contour lines (rather than the square root of the 'high' number of pixels in our DEM). By doing so, we assume there is no spatial autocorrelation between the contour lines, which is more appropriate than assuming that there is no spatial autocorrelation between individual pixels (Etzelmüller, 2000; Schiefer et al., 2007). The stochastic uncertainty, sometimes also termed as standard error, is finally included by multiplying the standard deviation (*STDEV*) by a factor 2 (*STDEV*, Table 3, column 6) (about 95% confidence interval), and dividing it by the root of the number of contour lines. For the SRTM X-band and the LIDAR DEM from 2010 we calculated the stochastic uncertainty by evaluating the *STDEV* of the elevation differences between the DEMs over stable terrain and n, the number of the evaluated cells (Koblet et al., 2010; Rolstad et al., 2009; Zemp et al., 2013).

$$\sigma = \frac{2 * \mathrm{STDEV}}{\sqrt{n}}$$

To assess glacier volume change uncertainties, we rely on a rather conservative approach and assume that the uncertainty in surface elevation changes is correlated. The uncertainty in the glacier-individual volume change is given by the *STDEV* after co-registration (Table 3, column 6) of the measured elevation differences (Cox and March, 2004; Larsen et al., 2007). The *STDEV* is multiplied by the area of the corresponding year in Table 4.

4.3. Data preparation for computer animation

4.3.1. DEM preparation

For the computer animation, we filled all data voids visible in the DEMs of the Siegfried maps and the Dufour map (Fig. 4). Areas with data voids, mostly visible in exposed zones like the tongue of Adlergletscher but also in the accumulation area of Findelengletscher (Fig. 5), were filled with the DEM values from the year 1937 as this map represents the first accurate map for glaciological purposes.

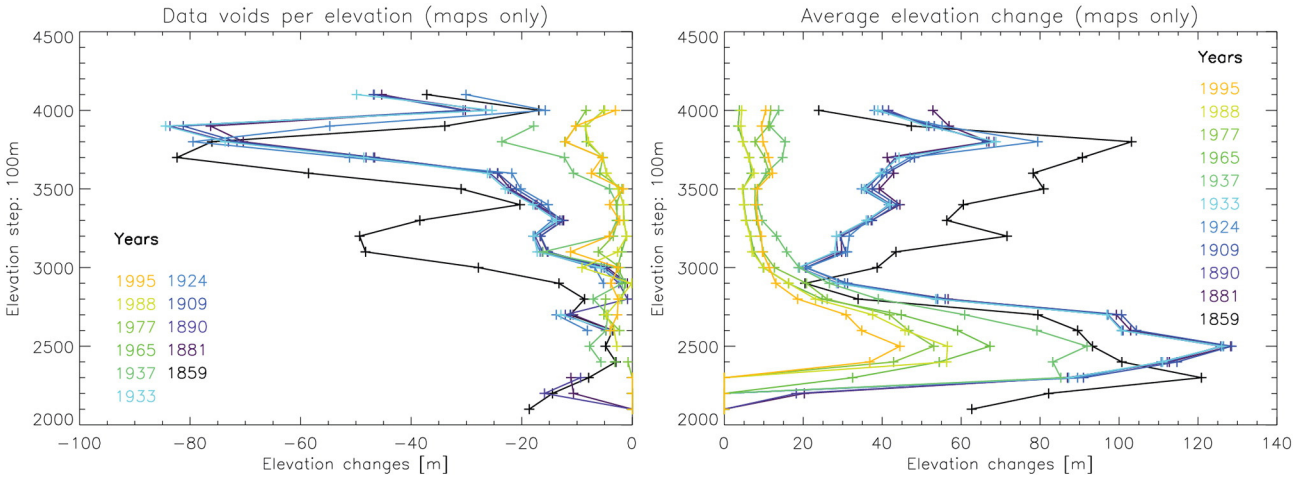

Fig. 4. Data voids (left) and average elevation differences relative to 2005 (right) per elevation interval for all map derived DEMs.

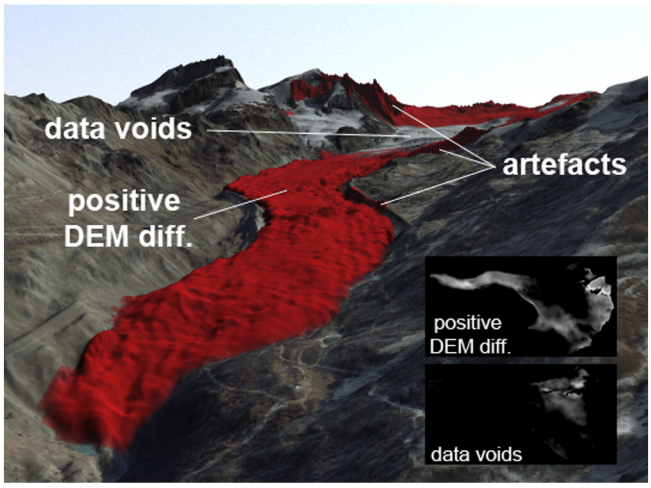

Fig. 5. Visualized DEM differences showing the data voids and artefacts between the DEM from 1859 and the laser scanning DEM from 2005 (raw DEMs are shown in inset).

In a next step, the historical DEMs were adjusted to the current terrain by slightly blurring the glacier margin (brush tool) in Adobe Photoshop (Fig. 5). This was necessary as due to glacier retreat the lateral slopes began to erode (Ballantyne, 2002), leading to smoother slopes.

4.3.2. DEM sequence

After the void filling of the first six DEMs and artefact correction of all historical DEMs, a DEM sequence had to be calculated, which was used in each frame (individual images of an animation) for rendering (calculating frames using parameter settings in VNS) (3D Nature, 2003). Based on experience, a duration of ~35 s for such an animation is feasible, which results in 906 frames in total (6 per year). The morphing (special effect in motion pictures that changes one image into another through a seamless transition) itself was performed by first defining the amount of DEMs to be interpolated from one reference year to the next one and then selecting reference points in each DEM to steer the morph direction.

4.3.3. Glacier extent reference lines and time line

The most prominent glacier extents (1859, 1881, 1909, 1937, 1965, 1977, 1988, and 2000) were also included in the animation as reference (Fig. 7, right). The respective glacier outlines were converted from a shape file to a raster file with a line width of four pixels and saved as a Truevision Advanced Raster Graphics Array (TARGA) file with an alpha channel (image band that stores the transparency information of an image). The time line (Fig. 7, a & b) was created in Photoshop using three layers.

4.4. Rendering and movie editing

The reference DEM, resampled to 8 m pixel size, served as a base for the animation. This ensures enough terrain naturalism in the animation and additionally increases the speed for rendering. To increase the realism of the current landscape, the orthophoto from October 2005 was resampled to 5 m and draped on the reference DEM. To simulate the historical landscape, the VNS function "area terrafector" (unique displacement effects in VNS which can change the shape of the terrain) was applied (3D Nature, 2003). This function allows changes of the reference DEM according to an input image (DEM sequence). Subsequently, a good camera position with a panoramic perspective was found to render the animation. The last step, the video authoring, was performed in Adobe Premiere by assembling the computer animation with the animated time line. Finally, a title, an introductory slide and a trailer with all credits at the end of the animation were inserted.

5. Results

5.1. Length-, area-, thickness- and volume changes of Findelengletscher

The length of Findelengletscher was 10.43 km in 1859 and decreased to 6.90 km (−3.53 km) by 2010 (Table 4). At the same time, the glacier area decreased from 19.47 ± 0.58 km^2 in 1859 to 15.05 ± 0.45 km^2 (−4.42 ± 0.13 km^2), respectively to 13.03 ± 0.40 km^2 without the area of Adlergletscher in 2010. Since 1859, the glacier showed a general retreat which was interrupted in the 1890s, and 1980s, which is also supported by direct measurements of the annual length change at the glacier snout (Glaciological reports (1881–2016), 2016). In the 1970s, the glacier below Strahlhorn (Fig. 1, marked with an x) separated from Findelengletscher and around 1990 Adlergletscher detached. After the last area increase during the 1980s the glacier system lost 0.44 ± 0.01 km^2 of its area between 1988 and 1995 and 1.38 ± 0.04 km^2 in the period 1995 to 2010.

The average rate of thickness loss is 0.45 ± 0.042 m yr^{-1} for the whole study period. Four periods with higher thickness change of −0.56 ± 0.28 m yr^{-1} (1859–1881), −0.40 ± 0.08 m yr^{-1} (1937–1965), −0.90 ± 0.31 m yr^{-1} (1995–2000) and −1.18 ± 0.02 m yr^{-1} (2000–2005) have been identified. Small positive thickness changes were found for the periods 1890–1909 (+0.09 ± 0.46 m yr^{-1}) and 1988–1995 (+0.05 ± 0.24 m yr^{-1}) (Table 5 and Fig. 6).

Table 5
Average thickness changes from one input dataset to the next with systematic and stochastic uncertainties. $\overline{dh}_{glacierized}$: differences from one DEM to the next one over glacierized terrain, ϵ: mean differences from one DEM to the next one over stable terrain; $\overline{dh} + \epsilon \pm \sigma$ is the corrected mean glacierized thickness change and its stochastic uncertainty. Note: the independent DEM from 1982 shows absolute thickness changes from 1982 to 2005.

Year periods	$\overline{dh}_{glacierized}$ dataset to dataset [m]	ϵ [m]	$\overline{dh} + \epsilon$ [m]	$\overline{dh}_{glacierized} + \epsilon \pm \sigma$ [m]
1859–1881	−13.3	0.8	−12.5	−12.5 ± 6.25
1881–1890	−1.9	0.06	−1.84	−1.84 ± 8.83
1890–1909	0.7	1.13	1.83	1.83 ± 8.90
1909–1924	−0.4	1.64	1.24	1.24 ± 9.35
1924–1933	−1.5	1.8	0.14	0.14 ± 9.44
1933–1937	−20.4	0.29	−20.11	−20.11 ± 9.01
1937–1965	−11.5	0.21	−11.29	−11.29 ± 2.44
1965–1977	−1.2	1.08	−0.12	−0.12 ± 1.57
1977–1988	−1.8	1.06	−0.74	−0.74 ± 1.70
1988–1995	−0.7	1.05	0.35	0.35 ± 1.69
1995–2000	−5.9	1.27	−4.63	−4.63 ± 1.56
2000–2005	−5.8	−0.13	−5.93	−5.93 ± 0.14[a]
2005–2010	−3.4	0.22	−3.18	−3.18 ± 0.2[a]
1982 ind. DEM – 2005	−13.4	0.14	−13.26	−13.26 ± 3.4[a]

[a] All pixel values with co-registration.

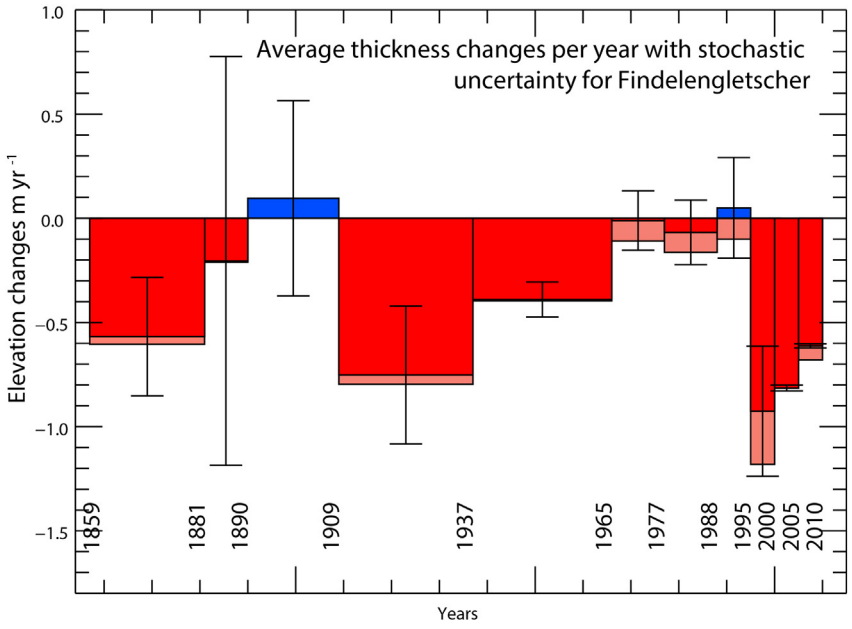

Fig. 6. Average thickness changes per year (effective changes are shown in dark red, in light red erroneous thickness changes and positive ones in blue) with applied stochastic uncertainties as calculated in Table 5. The values stemming from the maps of 1924 and 1933 were removed as they basically depict the status of 1909.

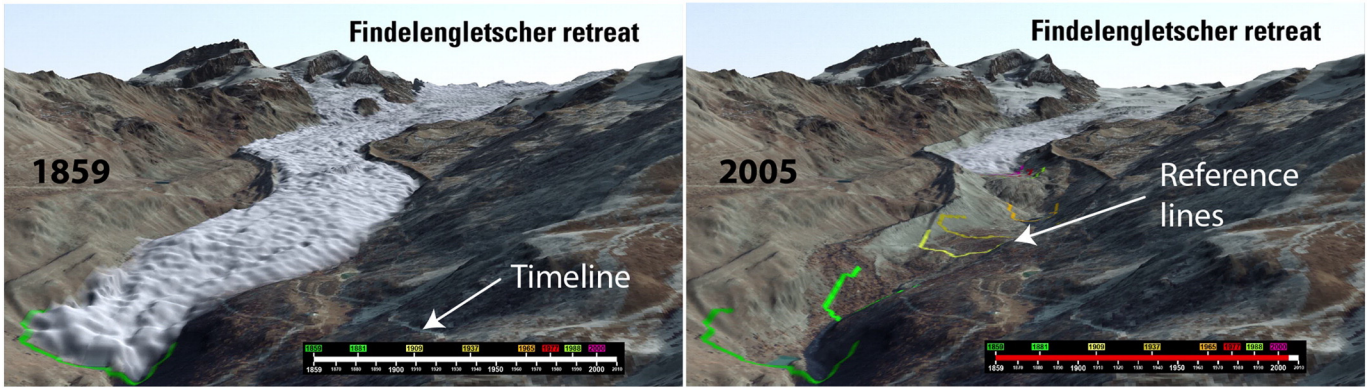

Fig. 7. Extent of Findelengletscher in 1859 and 2005 based on historic maps and airborne laser scanning. The lines in the glacier forefield represent the historic glacier extent.

5.2. Visualizations and exhibition stand

Our compilation of digital historical map data resulted in a computer animation, which shows the spatio-temporal changes in Findelengletscher from 1859 to 2010 (see computer animation in the supplement). The reconstruction of Findelengletscher in 1859 illustrates that the glacier shrank already before due to the fact that the glacier surface is mapped lower than the lateral moraines stemming from the LIA (Sommer, 1988). During the retreat, coloured outlines in the front emerge, indicating the glacier extent in the respective year. In the bottom of the movie, a time line is displaying the year shown in the animation. The advance of the glacier tongue during the 1980s and the disconnection of Adlergletscher in the beginning of the 1990s is clearly visible.

In cooperation with professional booth builders, the animation was used as the central part in a glacier exhibit stand (Fig. 8). On a large touch screen the animation of Findelengletscher is shown, and the visitor can travel through time by touching the monitor and dragging the glacier tongue forward or backward. This main screen is embedded into a large panoramic view, which shows the Zermatt valley with the Monte Rosa Mountains. For visitors with an additional interest for the topic, another interactive monitor located next to the panoramic view provides related background information in French and German. In 2013, the glacier exhibit was launched as permanent part of a visitor centre and is ready for more than 10,000 visitors a year.

Fig. 8. Exhibition stand at the Axporama visitor centre, Böttstein, Switzerland.

6. Discussion

6.1. Glacier changes

The numbers for length, area and volume changes presented here are difficult to compare with other studies. This is because in many cases, the time periods are different, a co-registration has not been performed or the resolution of the DEMs were different. The calculated numbers of length-, area- and volume changes along with the animation confirm strong retreat and mass loss of Findelengletscher since the mid-19th century. Maisch et al. (2000) presented slightly different data for the length and area of Findelengletscher in 1850. In their publication, a length of 10.40 km and an area of 19.95 km^2 is provided (this study: 10.43 km and 19.47 ± 0.58 km^2). The total glacier area decreased by ~23% from 1859 to 2010 at annual rates increasing from 0.15% yr^{-1} in the beginning of the measurements to 0.30% yr^{-1} from 1965 on, and to 0.56% yr^{-1} from 1995 to 2010.

The increasing trend is also in line with the average thickness changes of Findelengletscher (cumulative signal is significantly negative). The annual thickness changes are increasing from 1850 to the present and the phases with strong loss are all significantly negative. All the other periods are close to zero balances and have a relatively high uncertainty. The latter is a result of the noise in the DEMs and depends also on the amount of contour lines taken to calculate the stochastic uncertainty. The Findelengletscher's mean elevation change per year was from 1859 to 2010 was −0.45 ± 0.042 m yr^{-1}. The numbers are in accordance with Unterer Grindelwaldgletscher that showed an average thickness change of −0.42 m yr^{-1} (1860–2004) and Unteraargletscher an average thickness change −0.48 m yr^{-1} (Steiner et al., 2008). The averages thickness changes per year are consistent with an integrated assessment of long-term in situ measurements, satellite images, digital terrain information and numerical models (Haeberli et al., 2007), where a mean annual thickness change of −0.43 m ± 0.24 m from 1890 to 1999 was estimated. We also used the independent DEM from 1982 of Findelengletscher from Bauder et al. (2007). After co-registration with the master DEM, we calculated the mean thickness change of −13.2 ± 3.4 m from 1982 to 2005. The comparison of the change rates of 1977–2005 (DEM from this study) and 1982–2005 (DEM from Bauder et al., 2007) gives exactly the same value of −0.57 m yr^{-1} in both cases. The mean geodetic mass balance of Findelengletscher, assuming a density of 850 ± 60 kg/m^{-3} (Huss, 2013), for the whole study time, is −0.38 m water equivalent (w.e.) per year. This number is higher (along with our study period) than the arithmetic mean (−0.29 m w.e. yr^{-1}) of 20 glaciers in the southeastern Swiss Alps since 1900 presented in Huss et al. (2010). One can compare the total volume loss with the volume of the Cheops pyramid in Egypt. Dividing the volume loss (1.32 km^3) of Findelengletscher for the whole study period with the volume of the pyramid (0.00258 km^3) results in more than 510 Cheops pyramids.

6.2. Datasets and methods

This study has shown that co-registration of historically derived DEMs is required to obtain reasonable geodetic ice volume changes. A test with DEMs without co-registration revealed thickness changes which were about 5% and for the 1859 DEM about 30% larger. As consequence, the DEM from 1859 along with the SRTM X-band DEM products two iterations were necessary during the co-registration. A possible reason for the Dufour map derived DEM difference is attributable to the acquisition method (terrestrial survey), to the georeferencing with GCPs and to the overall lower accuracy due to the 30 m equidistance of the contour lines. In addition, the elevation adjustment from the "old horizon" to the "new horizon" (Δ −3 m) before the co-registration for 1859 was not relevant as compared to the overall uncertainty ($\epsilon > 40$ m). Interestingly, the co-registration method proposed by Nuth and Kääb (2011) does not eliminate the bias between two datasets as there is a remaining bias due to curve fitting. Theoretically, the vector sums should be zero for the horizontal and vertical components, but in practice residuals are present reflecting the method's uncertainty (Paul et al., 2015). Moreover, the SRTM X-band DEM exhibits a considerable elevation offset compared to all other independently derived DEMs (Table 4). This indicates a systematically too high surface topography (54.5 m) in the glacier-free area which is also confirmed by other studies (Kolecka and Kozak, 2014; Muskett et al., 2008). The reason for this is the vertical reference system (WGS84 ellipsoid) and not the quality of the DEM itself. In order to check whether the co-registration results are reliable we cross checked the SRTM X-band DEM mean elevation difference with the online "reframe tool", a Swisstopo's planimetric and altimetric transformation software for applications with the highest accuracy requirements. This cross check revealed a mean elevation difference of 54.9 m, which confirms that the co-registration corrected most of the geoid undulation. Moreover, it showed that the horizontal change in geoid undulation in the area of Findelengletscher was in the range of few centimeters per kilometer and thus a geoid undulation adjustment before co-registration was not necessary. However, we suggest always checking for the horizontal variability of the geoid undulation and, if necessary, correcting before the co-registration step.

The quality of the maps regarding contour lines elevations varies considerably in particular where snow/ice surface contrasts are expected to be low and/or in complex terrain (cf. Table 1 and Fig. 4). Suspicious thickness changes in particular in the accumulation region of historical maps were also reported by other authors (Bris and Paul, 2015; Steiner et al., 2008). Steiner et al. (2008) analyzed surface elevation changes on Fiescherglletscher in the Bernese Alps over the past two centuries. He attributes the lower surface of the past in the accumulation region to changes in glacier dynamics and not to a lack of in-situ measurements in the upper part of the glacier, which is relatively flat and thus difficult to survey. Bauder et al. (2007) highlight the issue of having fewer problems regarding DEM accuracy on glaciers where larger changes occur. Our results confirm this interpretation, as map updates were usually only made when large changes occurred. This drawback of quality is inherent in the maps and not a result of the contour line method. Using another approach to calculate thickness and volume changes, like relying on single vertexes (Kääb, 2008; Nuth et al., 2007) and not on the contour line method, would still lead to such an inconsistency. Our method to calculate elevation changes, by accounting only average thickness values for each elevation bin, may also, like data voids, be prone to biases (Table 1 and Fig. 3). With the help of reference ground points, we did, however, not find any distinctive tilt or tilt axes of the maps neither before 1937 nor after. We therefore conclude that our method regarding the contour line method and the hypsometric thickness change calculation provide reasonable accurate results even with a DEM raster resolution of 25 × 25 m (cf. Joerg and Zemp, 2014).

Besides that, there are other uncertainties in our data like reliable reference points through time for the georeferencing or the inconsistent updates of the glacier outlines respectively the contour lines. In the three maps from 1909 to 1933, for example, there is nearly no glacier change detectable (Tables 1 and 4). Hence, the large elevation change from 1933 to 1937 as the map from 1933 depicts the state of the glacier from 1909. As this sudden large glacier volume change is misleading, we removed the years (1924 & 1933) in Fig. 6 and provided corrected values (−0.75 ± 0.30 m yr^{-1}) for the 1909–1937 period. For calculating the rate of glacier elevation change, the available accuracy is thus often insufficient. However, the dating of maps after the late 1930s satisfies the required accuracy and is of unique value for glaciological reconstruction of former surface topography.

6.3. Visualization

Visualizing the present situation is relatively simple by taking existing data and combining it with modern technology. Conversely, visualizing historic glacier fluctuations is difficult unless relevant data

(Wang et al., 2006) or 3D flow models are used (Jouvet et al., 2011, 2009). In Switzerland, the availability of accurate and periodically updated data in the form of maps with elevation contour lines represents a unique opportunity to explore past glacier extents. The transferability of this study is therefore limited and might not be possible to the same degree in other remote high alpine regions.

A drawback of the animation is the linear change of the glacier geometry between two DEMs, which is not the case in reality. Including time series of measured length changes might help to increase the realism of the simulation. Moreover, at a 25 m DEM resolution the glacier surface is rather blocky and rough. This is foremost a drawback of VNS "area terrafector" which is unable to import signed-float imageries. To make the animation more appealing, DEMs with a higher spatial resolution should be used as the higher resolution removes the well visible rectangular pixels in the animation. However, the here presented method to visualize landscape evolution is not only applicable for glacier changes but also for any other slope related movements which affect the terrain considerably. By whatever means researchers are able to show in landscape evolution, we conclude that 3D animations are a promising tool for visualizing landscape changes through time for a wider public.

7. Conclusion

We have presented a way to transform glacier extents from historic topographic maps into (a) scientific products like changes in length, area and volume of Findelengletscher since 1859 and (b) informative products for public communication including a computer animation. Eleven historical maps, dating back to 1859, in combination with the SRTM X-band DEM and laser-scanning DEMs were used for this purpose. The pre-processing stressed the importance of co-registration to avoid systematic uncertainties in glacier volume changes. From 1859 to 2010, Findelengletscher lost 3.5 km of its length (6.90 km in 2010), 4.42 ± 0.13 km^2 of its area (15.05 ± 0.46 km^2 in 2010) and 1.32 ± 0.52 km^3 of its volume, but the rates of change varied considerably during the investigated period. The average thickness loss rate was 0.45 ± 0.042 m yr^{-1} for the entire period. Around the 1920s and 1980s, glacier shrinkage was limited but from the 1960s and 1990s onwards, high melt rates are visible, consistent with the signal of other glaciers in the Swiss Alps. The whole evolution of the Findelenglacier is visualized in a computer animation that is downloadable in the supplementary material of this article and can be used for scientific or educational purposes.

Supplementary data to this article can be found online at http://dx.doi.org/10.1016/j.gloplacha.2016.07.005.

Acknowledgements

This work was supported by the Glacier Laser Scanning Project Oberwallis (GLAXPO) of the Swiss energy company Axpo in collaboration with the Department of Geography at the University of Zurich and the European Space Agency Glaciers_cci project (4000109873/14/I-NB). We thank Swisstopo for providing all the historical maps. Landsat data was downloaded from the USGS Earth Explorer (http://earthexplorer.usgs.gov/) and the SRTM DEM from DLR EOWEB (https://centaurus.caf.dlr.de:8443/eoweb-ng/template/default/welcome/entryPage.vm.) We are grateful for the constructive comments from the reviewers and of Frank Paul. Moreover, we want to thank Marc de Souza for proof reading the paper and thank the visitor centre Axporama for implementing the glacier exhibit.

References

3D Nature, 2003. Visual Nature Studio 2. Using VNS. Professional Photorealistic Terrain Visualization, Modeling, Rendering & Animation Software.
Ballantyne, C.K., 2002. Paraglacial geomorphology. Quat. Sci. Rev. 21, 1935–2017. http://dx.doi.org/10.1016/S0277-3791(02)00005-7.
Bauder, A., Funk, M., Huss, M., 2007. Ice-volume changes of selected glaciers in the Swiss Alps since the end of the 19th century. Ann. Glaciol 46, 145–149.
Bolch, T., Menounos, B., Wheate, R., 2010. Landsat-based inventory of glaciers in western Canada, 1985–2005. Remote Sens. Environ 114, 127–137.
Bris, R.L., Paul, F., 2015. Glacier-specific elevation changes in parts of western Alaska. Ann. Glaciol 56, 184–192. http://dx.doi.org/10.3189/2015AoG70A227.
Cox, L.H., March, R.S., 2004. Comparison of geodetic and glaciological mass-balance techniques, Gulkana Glacier, Alaska, USA. J. Glaciol 50, 363–370.
Dehecq, A., Millan, R., Berthier, E., Gourmelen, N., Trouvé, E., 2016. Elevation changes inferred from TanDEM-X data over the Mont-Blanc area: Impact of the X-band interferometric bias. Journal of selected topics in applied earth observations and remote sensing 99. http://dx.doi.org/10.1109/JSTARS.2016.2581482.
Etzelmüller, B., 2000. On the quantification of surface changes using gridbased Digital Elevation Models (DEMs). Trans. GIS 4 (2), 129–143.
Farr, T.G., Rosen, P.A., Caro, E., Crippen, R., Duren, R., Hensley, S., Kobrick, M., Paller, M., Rodriguez, E., Roth, L., Seal, D., Shaffer, S., Shimada, J., Umland, J., Werner, M., Oskin, M., Burbank, D., Alsdorf, D., 2007. The shuttle radar topography mission. Rev. Geophys 45. http://dx.doi.org/10.1029/2005RG000183.
Finsterwalder, R., Rentsch, H., 1980. Zur Höhenänderung von Ostalpengletschern im Zeitraum 1969-1979. Z. Gletscherk. Glazialgeol 16 (1), 111–115.
Fischer, A., 2011. Comparison of direct and geodetic mass balances on a multi-annual time scale. The Cryosphere 5, 107–124. http://dx.doi.org/10.5194/tc-5-107-2011.
Gardelle, J., Berthier, E., Arnaud, Y., Kääb, A., 2013. Region-wide glacier mass balances over the Pamir-Karakoram-Himalaya during 1999–2011. The Cryosphere 7, 1263–1286. http://dx.doi.org/10.5194/tc-7-1263-2013.
Glaciological Reports (1881–2016), 2016. The Swiss glaciers. Yearbooks of the Cryospheric Commission of the Swiss Academy of Sciences (SCNAT) Published Since 1964 by the Labratory of Hydraulics, Hydrology and Glaciology (VAW) of ETH Zürich. No. 1–134, pp. 1–134 (http://glaciology.ethz.ch/swiss-glaciers/).
Graf, J.H., 1896. Die schweizerische Landesvermessung 1832–1864. Geschichte der Dufourkarte, Zürich.
Gubler, E., 2011. 150 Jahre Schweizerische Geodätische Kommission. Géomatique Suisse 6, 260–268.
Haeberli, W., Hoelzle, M., Paul, F., Zemp, M., 2007. Integrated monitoring of mountain glaciers as key indicators of global climate change: the European Alps. Ann. Glaciol 46, 150–160.
Haggren, H., Mayer, C., Nuikka, M., Braun, L., Rentsch, H., Peipe, J., 2007. Processing of old terrestrial photography for verifying the 1907 digital elevation model of Hochjochferner glacier. Z. Gletscherk. Glazialgeol 41, 29–54.
Hoffmann, J., Walter, D., 2006. How complementary are SRTM-X and-C band digital elevation models? Photogramm. Eng. Remote. Sens. 72, 261–268.
Hoinkes, H., 1970. Methoden und Möglichkeiten von Massenhaushaltsstudien auf Gletschern. Z. Gletscherk. Glazialgeol 6, 37–90.
Holzhauser, H., 2010. Zur Geschichte des Gornergletschers: Ein Puzzle aus historischen Dokumenten und fossilen Hölzern aus dem Gletschervorfeld., Geographica Bernensia. ed.
Huss, M., 2013. Density assumptions for converting geodetic glacier volume change to mass change. The Cryosphere 7, 877–887. http://dx.doi.org/10.5194/tc-7-877-2013.
Huss, M., Usselmann, S., Farinotti, D., Bauder, A., 2010. Glacier mass balance in the south-eastern Swiss Alps since 1900 and perspectives for the future. Erdkunde 2010, 119–140. http://dx.doi.org/10.3112/erdkunde.2010.02.02.
Huss, M., Zemp, M., Joerg, P.C., Salzmann, N., 2014. High uncertainty in 21st century runoff projections from glacierized basins. J. Hydrol 510, 35–48. http://dx.doi.org/10.1016/j.jhydrol.2013.12.017.
Jarvis, A., Reuter, A., Nelson, E., Guevara, E., 2008. Hole-filled SRTM for the Globe Version. p. 4.
Joerg, P.C., Zemp, M., 2014. Evaluating volumetric glacier change methods using airborne laser scanning data. Geogr. Ann., Ser. A, Phys. Geogr 96, 135–145. http://dx.doi.org/10.1111/geoa.12036.
Joerg, P.C., Morsdorf, F., Zemp, M., 2012. Uncertainty assessment of multi-temporal airborne laser scanning data: a case study on an Alpine glacier. Remote Sens. Environ 127, 118–129. http://dx.doi.org/10.1016/j.rse.2012.08.012.
Jouvet, G., Huss, M., Blatter, H., Picasso, M., Rappaz, J., 2009. Numerical simulation of Rhonegletscher from 1874 to 2100. J. Comput. Phys 228, 6426–6439. http://dx.doi.org/10.1016/j.jcp.2009.05.033.
Jouvet, G., Huss, M., Funk, M., Blatter, H., 2011. Modelling the retreat of Grosser Aletschgletscher, Switzerland, in a changing climate. J. Glaciol 57, 1033–1045.
Junfeng, W., Shiyin, L., Wanqin, G., Junli, X., Weijia, B., Donghui, S., 2015. Changes in glacier volume in the north bank of the Bangong Co Basin from 1968 to 2007 based on historical topographic maps, SRTM, and ASTER stereo images. Arct. Antarct. Alp. Res 47, 301–311. http://dx.doi.org/10.1657/AAAR00C-13-129.
Kääb, A., 2008. Glacier volume changes using ASTER satellite stereo and ICESat GLAS laser altimetry. A test study on Edgeøya, Eastern Svalbard. IEEE Trans. Geosci. Remote Sens 46, 2823–2830. http://dx.doi.org/10.1109/TGRS.2008.2000627.
Koblet, T., Gärtner-Roer, I., Zemp, M., Jansson, P., Thee, P., Haeberli, W., Holmlund, P., 2010. Reanalysis of multi-temporal aerial images of Storglaciären, Sweden (1959–99) – part 1: determination of length, area, and volume changes. The Cryosphere 4, 333–343. http://dx.doi.org/10.5194/tc-4-333-2010.
Kobold, F., 1983. Von den Anfängen der schweizerischen Landesvermessung 1809–1840. Vermessung, Photogrammetrie, Kulturtechnik: VPK = Mensuration, photogrammétrie, génie rural, p. 9.
Kolecka, N., Kozak, J., 2014. Assessment of the accuracy of SRTM c- and x-band high mountain elevation data: a case study of the Polish Tatra Mountains. Pure Appl. Geophys 171, 897–912. http://dx.doi.org/10.1007/s00024-013-0695-5.
Larsen, C.F., Motyka, R.J., Arendt, A.A., Echelmeyer, K.A., Geissler, P.E., 2007. Glacier changes in southeast Alaska and northwest British Columbia and contribution to sea level rise. J. Geophys. Res 112. http://dx.doi.org/10.1029/2006JF000586.

Machguth, H., 2008. On the use of RCM data and gridded climatologies for regional scale glacier mass balance modeling in high mountain topography. The Example of the Swiss Alps. Zürich, Zürich.

Machguth, H., Huss, M., 2014. The length of the world's glaciers - a new approach for the global calculation of center lines. The Cryosphere 8, 1741–1755. http://dx.doi.org/10.5194/tc-8-1741-2014.

Maisch, M., Wipf, A., Denneler, B., Battaglia, J., Benz, C., 2000. Die Gletscher der Schweizer Alpen: Gletscherhochstand 1850, Aktuelle Vergletscherung, Gletscherschwund-Szenarien. 2. vdf, Hochsch.-Verlag an der ETH, Zürich.

Muskett, R.R., Lingle, C.S., Sauber, J.M., Rabus, B.T., Tangborn, W.V., 2008. Acceleration of surface lowering on the tidewater glaciers of Icy Bay, Alaska, U.S.A. from InSAR DEMs and ICESat altimetry. Earth Planet. Sci. Lett 265, 345–359. http://dx.doi.org/10.1016/j.epsl.2007.10.012.

Nuth, C., Kääb, A., 2011. Co-registration and bias corrections of satellite elevation data sets for quantifying glacier thickness change. Cryosphere 5, 271–290. http://dx.doi.org/10.5194/tc-5-271-2011.

Nuth, C., Kohler, J., Aas, H.F., Brandt, O., Hagen, J.O., 2007. Glacier geometry and elevation changes on Svalbard (1936–90): a baseline dataset. Ann. Glaciol 46, 106–116. http://dx.doi.org/10.3189/172756407782871440.

Oberli, A., 1968. Vor 100 Jahren: Wie es zur Herausgabe der Siegfriedkarten kam. Hauszeitung der Eidg. Landestopographie (Wabern). Vol. 23, pp. 7–22.

Paul, F., Haeberli, W., 2008. Spatial variability of glacier elevation changes in the Swiss Alps obtained from two digital elevation models. Geophys. Res. Lett 35, L21502. http://dx.doi.org/10.1029/2008GL034718.

Paul, F., Barrand, N.E., Baumann, S., Berthier, E., Bolch, T., Casey, K., Frey, H., Joshi, S.P., Konovalov, V., Bris, R.L., Mölg, N., Nosenko, G., Nuth, C., Pope, A., Racoviteanu, A., Rastner, P., Raup, B., Scharrer, K., Steffen, S., Winsvold, S., 2013. On the accuracy of glacier outlines derived from remote-sensing data. Ann. Glaciol 54, 171–182. http://dx.doi.org/10.3189/2013AoG63A296.

Paul, F., Bolch, T., Kääb, A., Nagler, T., Nuth, C., Scharrer, K., Shepherd, A., Strozzi, T., Ticconi, F., Bhambri, R., Berthier, E., Bevan, S., Gourmelen, N., Heid, T., Jeong, S., Kunz, M., Lauknes, T.R., Luckman, A., Merryman Boncori, J.P., Moholdt, G., Muir, A., Neelmeijer, J., Rankl, M., VanLooy, J., Van Niel, T., 2015. The glaciers climate change initiative: methods for creating glacier area, elevation change and velocity products. Remote Sens. Environ 113, 1–19. http://dx.doi.org/10.1016/j.rse.2013.07.043.

Rastner, P., Bolch, T., Mölg, N., Machguth, H., Le Bris, R., Paul, F., 2012. The first complete inventory of the local glaciers and ice caps on Greenland. The Cryosphere 6, 1483–1495. http://dx.doi.org/10.5194/tc-6-1483-2012.

Rickenbacher, M., 2009. Napoleons Karten der Schweiz: Landesvermessung als Machtfaktor zwischen 1798 und 1815. University of Basel.

Rignot, E., Echelmeyer, K., Krabill, W., 2001. Penetration depth of interferometric synthetic-aperture radar signals in snow and ice. Geophys. Res. Lett 28, 3501–3504. http://dx.doi.org/10.1029/2000GL012484.

Rolstad, C., Haug, T., Denby, B., 2009. Spatially integrated geodetic glacier mass balance and its uncertainty based on geostatistical analysis: application to the western Svartisen ice cap, Norway. J. Glaciol 55, 666–680.

Schiefer, E., Menounos, B., Wheate, R., 2007. Recent volume loss of British Columbian glaciers, Canada. Geophys. Res. Lett 34, L16503. http://dx.doi.org/10.1029/2007GL030780.

Sold, L., Huss, M., Hoelzle, M., Andereggen, H., Joerg, P.C., Zemp, M., 2013. Methodological approaches to infer end-of-winter snow distribution on alpine glaciers. J. Glaciol 59, 1047–1059. http://dx.doi.org/10.3189/2013JoG13J015.

Sold, L., Huss, M., Machguth, H., Joerg, P.C., Leysinger Vieli, G., Linsbauer, A., Salzmann, N., Zemp, M., Hoelzle, M., 2016. Mass balance re-analysis of Findelengletscher, Switzerland; benefits of extensive snow accumulation measurements. Frontiers in Earth Science 4, 18. http://dx.doi.org/10.3389/feart.2016.00018.

Sommer, I., 1988. Gletschergeschichtliche Untersuchungen und dendrochronologische Analysen an Lärchen (*Larix decidua* Mill.) im Val Ferret und im Raum Zermatt, VS (Glacier de Saleina, Glacier de l'A Neuve und Findelengletscher). University of Zurich, Zurich.

Steiner, D., Zumbühl, H.J., Bauder, A., 2008. Two Alpine glaciers over the past two centuries: a scientific view based on pictorial sources. Darkening Peaks: Glacier Retreat, Science, and Society. University of California Press, Berkeley, pp. 83–99.

Surazakov, A.B., Aizen, V.B., 2006. Estimating volume change of mountain glaciers using SRTM and map-based topographic data. IEEE Trans. Geosci. Remote Sens 44, 2991–2995. http://dx.doi.org/10.1109/TGRS.2006.875357.

Wang, X., Song, B., Chen, J., Zheng, D., Crow, T.R., 2006. Visualizing forest landscapes using public data sources. Landsc. Urban Plan 75, 111–124. http://dx.doi.org/10.1016/j.landurbplan.2004.12.010.

Wolf, J.R., 1879. Geschichte der Vermessungen der Schweiz. Commission von S. Höhr, Zürich.

Xu, J., Liu, S., Zhang, S., Guo, W., Wang, J., 2013. Recent changes in glacial area and volume on Tuanjiefeng peak region of Qilian Mountains, China. PLoS One 8, e70574. http://dx.doi.org/10.1371/journal.pone.0070574.

Zemp, M., Thibert, E., Huss, M., Stumm, D., Rolstad Denby, C., Nuth, C., Nussbaumer, S.U., Moholdt, G., Mercer, A., Mayer, C., Joerg, P.C., Jansson, P., Hynek, B., Fischer, A., Escher-Vetter, H., Elvehøy, H., Andreassen, L.M., 2013. Reanalysing glacier mass balance measurement series. The Cryosphere 7, 1227–1245. http://dx.doi.org/10.5194/tc-7-1227-2013.